Unsupervised and Transfer Learning Challenge: a Deep Learning Approach

Grégoire Mesnil[1,2] MESNILGR@IRO.UMONTREAL.CA
Yann Dauphin[1] DAUPHIYA@IRO.UMONTREAL.CA
Xavier Glorot[1] GLOROTXA@IRO.UMONTREAL.CA
Salah Rifai[1] RIFAISAL@IRO.UMONTREAL.CA
Yoshua Bengio[1] BENGIOY@IRO.UMONTREAL.CA
Ian Goodfellow[1] GOODFELI@IRO.UMONTREAL.CA
Erick Lavoie[1] LAVOERIC@IRO.UMONTREAL.CA
Xavier Muller[1] MULLERX@IRO.UMONTREAL.CA
Guillaume Desjardins[1] DESJAGUI@IRO.UMONTREAL.CA
David Warde-Farley[1] WARDEFAR@IRO.UMONTREAL.CA
Pascal Vincent[1] VINCENTP@IRO.UMONTREAL.CA
Aaron Courville[1] COURVILA@IRO.UMONTREAL.CA
James Bergstra[1] BERGSTRJ@IRO.UMONTREAL.CA
[1] *Dept. IRO, Université de Montréal. Montréal (QC), H2C 3J7, Canada*
[2] *LITIS EA 4108, Université de Rouen. 76 800 Saint Etienne du Rouvray, France*

Editor: I. Guyon, G. Dror, V. Lemaire, G. Taylor, and D. Silver

Abstract

Learning good representations from a large set of unlabeled data is a particularly challenging task. Recent work (see Bengio (2009) for a review) shows that training deep architectures is a good way to extract such representations, by extracting and disentangling gradually higher-level factors of variation characterizing the input distribution. In this paper, we describe different kinds of layers we trained for learning representations in the setting of the Unsupervised and Transfer Learning Challenge. The strategy of our team won the final phase of the challenge. It combined and stacked different one-layer unsupervised learning algorithms, adapted to each of the five datasets of the competition. This paper describes that strategy and the particular one-layer learning algorithms feeding a simple linear classifier with a tiny number of labeled training samples (1 to 64 per class).

Keywords: Deep Learning, Unsupervised Learning, Transfer Learning, Neural Networks, Restricted Boltzmann Machines, Auto-Encoders, Denoising Auto-Encoders.

1. Introduction

The objective of machine learning algorithms is to discover statistical structure in data. In particular, *representation-learning algorithms* attempt to transform the raw data into a form from which it is easier to perform supervised learning tasks, such as classification. This is particularly important when the classifier receiving this representation as input is linear and when the number of available labeled examples is small. This is the case here with the Unsupervised and Transfer Learning (UTL) Challenge [1].

Another challenging characteristic of this competition is that the training (development) distribution is typically very different from the test (evaluation) distribution, because it involves a set of classes different from the test classes, i.e., both inputs and labels have a different nature. What makes the task feasible is that these different classes have things in common. The bet we make is that *more abstract features of the data are more likely to be shared among the different classes*, even with classes which are very rare in the training set. Another bet we make with representation-learning algorithms and with Deep Learning algorithms in particular is that the structure of the input distribution $P(X)$ is strongly connected with the structure of the class predictor $P(Y|X)$ for all of the classes Y. It means that representations $h(X)$ of inputs X are useful both to characterize $P(X)$ and to characterize $P(Y|X)$, which we will think of as parametrized through $P(Y|h(X))$. Another interesting feature of this competition is that the input features are anonymous, so that teams are compared based on the strength of their learning algorithms and not based on their ability to engineer hand-crafted features based on task-specific prior knowledge. More material on Deep Learning can be found in a companion paper Bengio (2011).

The paper is organized as follows. The pipeline going from bottom (raw data) to top (final representation fed to the classifier) is described in Section 2. In addition to the score returned by the competition servers, Section 3 presents other criteria that guided the choice of hyperparameters. Section 4 precisely describes the layers we chose to combine for each of the five competition datasets, at the end of the exploration phase that lasted from January 2011 to mid-April 2011.

2. Method

We obtain a deep representation by stacking different single-layer blocks, each taken from a small set of possible learning algorithms, but each with its own set of hyper-parameters (the most important of which is often just the dimension of the representation). Whereas the number of possible combinations of layer types and hyper-parameters is exponential as depth increases, we used a greedy layer-wise approach (Bengio et al., 2007) for building each deep model. Hence, the first layer is trained on the raw input and its hyper-parameters are chosen with respect to the score returned by the competition servers (on the validation set) and different criteria to avoid overfitting to a particular subset of classes (discussed in Section 3). We then fix the i^{th} layer (or keep only a very small number of choices) and search for a good choice of the $i+1^{th}$ layer, pruning and keeping only a few good choices. Depth is thus increased without an explosion in computation until the model does not improve significantly the performance according to our criteria.

The resulting learnt pipeline can be divided in three types of stages: preprocessing, feature extraction and transductive postprocessing.

1. `http://http://www.causality.inf.ethz.ch/unsupervised-learning.php`

2.1. Preprocessing

Before the feature extraction step, we preprocessed the data using various techniques. Let $\mathcal{D} = \{x^{(j)}\}_{j=1,\ldots,n}$ be a training set where $x^{(j)} \in \mathbb{R}^d$.

Standardization One option is to standardize the data. For each feature, we compute its mean $\mu_k = (1/n)\sum_{j=1}^{n} x_k^{(j)}$ and variance σ_k. Then, each transformed feature $\tilde{x}_k^{(j)} = (x_k^{(j)} - \mu_k)/\sigma_k$ has zero mean and unit variance.

Uniformization (t-IDF) Another way to control the range of the input is to uniformize the feature values by restricting their possible values to $[0, 1]$ (and non-parametrically and approximately mapping each feature to a uniform distribution). We rank all the $x_k^{(j)}$ and map them to $[0, 1]$ by dividing the rank by the number of observations sorted. In the case of sparse data, we assigned the same range value (0) for zeros features. One option is to aggregate all the features in these statistics and another is to do it separately for each feature.

Contrast Normalization On datasets which are supposed to correspond to images, each input d-vector is normalized with respect to the values in the given input vector (global contrast normalization). For each sample vector $x^{(j)}$ subtract its mean $\mu^{(j)} = (1/d)\sum_{k=1}^{d} x_k^{(j)}$ and divide by its standard deviation $\sigma^{(j)}$ (also across the elements of the vector). In the case of images, this would discard the average illumination and contrast (scale).

Whitened PCA The Karhulen-Loève transform constantly improved the quality of the representation for each dataset. Assume the training set $\mathcal{D}$ is stored as a matrix $X \in \mathcal{M}_{\mathbb{R}}(n, d)$. First, we compute the empirical mean $\mu = (1/n)\sum_{i=1}^{n} X_{i.}$ where $X_{i.}$ denotes row i of the matrix X, i.e., example i. We center the data $\tilde{X} = X - \mu$ and compute the covariance matrix $C = (1/n)\tilde{X}^T\tilde{X}$. Then, we obtain the eigen-decomposition of the covariance matrix $C = V^{-1}UV$ i.e $U \in \mathbb{R}^d$ contains the eigen-values and $V \in \mathcal{M}_{\mathbb{R}}(d, d)$ the corresponding eigen-vectors (each row corresponds to an eigen-vector). We build a diagonal matrix U' where $U'_{ii} = \sqrt{C_{ii}}$. By the end, the output of the whitened PCA is given by $Y = (X - \mu)VU'$. In our experiments, we used the PCA implementation of the scikits [2] toolbox.

Feature selection In the datasets where the input is sparse, a preprocessing that we found very useful is the following: *only the features active on the training (development)* **and** *test (resp. validation) datasets are retained* for the test set (resp. validation) representations. We removed those whose frequency was low on both datasets (this introduces a new hyper-parameter that is the cut-off threshold, but we only tried a couple of values).

2.2. Feature extraction

Feature extraction is the core of our pipeline and has been crucial for getting the first ranks during the challenge. Here we briefly introduce each method that has been used during the competition. See also Bengio (2011) along with the citations below for more details.

2. http://scikits.appspot.com/

2.2.1. μ-ss-RBM

The μ-spike and slab Restricted Boltzmann Machine (μ-ssRBM) (Courville et al., 2011) is a recently introduced undirected graphical model that has demonstrated some promise as a model of natural images. The model is characterized by having both a real-valued *slab* vector and a binary *spike* variable associated with each hidden unit. The model possesses some practical properties such as being amenable to block Gibbs sampling as well as being capable of generating similar latent representations of the data to the mean and covariance Restricted Boltzmann Machine (Ranzato and Hinton, 2010).

The μ-ssRBM describes the interaction between three random vectors: the visible vector v representing the observed data, the binary "spike" variables h and the real-valued "slab" variables s. Suppose there are N hidden units and a visible vector of dimension D: $v \in \mathbb{R}^D$. The ith hidden unit ($1 \leq i \leq N$) is associated with a binary *spike* variable: $h_i \in \{0, 1\}$ and a real valued vector $s_i \in \mathbb{R}^K$, pooling over K linear filters. This kind of pooling structure allows the model to *learn* over which filters the model will pool – a useful property in the context of the UTL challenge where we cannot assume a standard "pixel structure" in the input. The μ-ssRBM model is defined via the energy function

$$
\begin{aligned}
E(v,s,h) = & -\sum_{i=1}^{N} v^T W_i s_i h_i + \frac{1}{2} v^T \left(\Lambda + \sum_{i=1}^{N} \Phi_i h_i \right) v \\
& + \sum_{i=1}^{N} \frac{1}{2} s_i^T \alpha_i s_i \ - \sum_{i=1}^{N} \mu_i^T \alpha_i s_i h_i - \sum_{i=1}^{N} b_i h_i + \sum_{i=1}^{N} \mu_i^T \alpha_i \mu_i h_i,
\end{aligned}
$$

in which W_i refers to the ith weight matrix of size $D \times K$, the b_i are the biases associated with each of the spike variables h_i, and α_i and Λ are diagonal matrices that penalize large values of $\|s_i\|_2^2$ and $\|v\|_2^2$ respectively.

Efficient learning and inference in the μ-ssRBM is rooted in the ability to iteratively sample from the factorial conditionals $P(h \mid v)$, $p(s \mid v, h)$ and $p(v \mid s, h)$ with a Gibbs sampling procedure. For a detailed derivation of these conditionals, we refer the reader to (Courville et al., 2011). In training the μ-ssRBM, we use stochastic maximum likelihood (Tieleman, 2008) to update the model parameters.

2.2.2. Denoising Autoencoder

Traditional autoencoders map an input $x \in \mathbb{R}^{d_x}$ to a hidden representation h (the learnt features) with an affine mapping followed by a non-linearity s (typically a sigmoid): $h = f(x) = s(Wx + b)$. The representation is then mapped back to input space, initially producing a linear reconstruction $r(x) = W' f(x) + b_r$, where W' can be the transpose of W (tied weights) or a different matrix (untied weights). The autoencoder's parameters $\theta = W, b, b_r$ are optimized so that the reconstruction is close to the original input x in the sense of a given loss function $L(r(x), x)$ (the reconstruction error). Common loss functions include squared error $\|r(x) - x\|^2$, squared error after sigmoid $\|s(r(x)) - x\|^2$, and sigmoid cross-entropy $-\sum_i x_i \log s(r_i(x)) + (1 - x_i) \log(1 - s(r_i(x)))$. To encourage robustness of the representation, and avoid trivial useless solutions, a simple and efficient variant was proposed in the form of the Denoising Autoencoders (Vincent et al., 2008, 2010). Instead of being trained to merely reconstruct its inputs, a Denoising Autoencoder is trained to *denoise* artificially corrupted training samples, a much more difficult task, which was shown to force it to extract more useful and meaningful features and capture the structure of the input distribution (Vincent et al., 2010). In practice, instead of presenting the encoder with a clean training sample x, it is given as input a stochastically corrupted version $\tilde{x}$. The objective remains to minimize reconstruction error $L(r(\tilde{x}), x)$ with respect to clean sample x, so that the hidden representation has to help denoise. Common choices for the corruption include additive Gaussian noise, and masking a fraction of the input components at random by setting them to 0 (masking noise).

2.2.3. Contractive Autoencoder

To encourage robustness of the representation $f(x)$ obtained for a training input x, Rifai et al. (2011) propose to penalize its *sensitivity* to that input, measured as the Frobenius norm of the Jacobian $J_f(x)$ of the non-linear mapping. Formally, if input $x \in \mathbb{R}^{d_x}$ is mapped by an encoding function f to a hidden representation $h \in \mathbb{R}^{d_h}$, this sensitivity penalization term is the sum of squares of all partial derivatives of the extracted features with respect to input dimensions:

$$\|J_f(x)\|_F^2 = \sum_{ij} \left(\frac{\partial h_j(x)}{\partial x_i} \right)^2 .$$

Penalizing $\|J_f\|_F^2$ encourages the mapping to the feature space to be contractive in the neighborhood of the training data. The *flatness* induced by having small first derivatives will imply an *invariance* or *robustness* of the representation for small variations of the input.

While such a Jacobian term alone would encourage mapping to a useless constant representation, it is counterbalanced in auto-encoder training by the need for the learnt representation to allow a good reconstruction of the training examples.

2.2.4. Rectifiers

Recent works investigated linear rectified activation function variants. Nair and Hinton (2010) used Noisy Rectified Linear Units (NReLU) (i.e. $\max(0, x+N(0, \sigma(x)))$ for Restricted Boltzmann Machines. Compared to binary units, they observed significant improvements in term of generalization performance for image classification tasks. Following this line of work, Glorot et al. (2011) used the rectifier activation function (i.e. $\max(0, x)$) for deep neural networks and Stacked Denoising Auto-Encoders (SDAE) (Vincent et al., 2008, 2010) and obtained similarly good results.

This non-linearity has various mathematical advantages. First, it naturally creates sparse representations with true zeros which are computationally appealing. In addition, the linearity on the active side of the activation function allows gradient to flow well on the active set of neurons, possibly reducing the vanishing gradients problem.

In a semi-supervised setting similar to that of the Unsupervised and Transfer learning Challenge setup, Glorot et al. (2011) obtained state-of-the-art results for a sentiment analysis task (the Amazon 4-task benchmark) for which the bag-of-words input were highly sparse.

But learning such embeddings for huge sparse vectors with the proposed approach is still very expensive. Even though the training cost only scales linearly with the dimension of the input, it can become too expensive when the input becomes very large. Projecting the input vector to its embedding can be made quite efficient by using a sparse matrix-vector product. However, projecting the embedding back to the input space is quite expensive during decoding because one has to compute a reconstruction (and reconstruction error) for all inputs and not just the non-zeros. If the input dimension is 50,000 and the embedding dimension 1,000 then decoding requires 50,000,000 operations. In order to speed-up training for huge sparse input distributions, we use reconstruction sampling (Dauphin et al., 2011). The idea is to reconstruct all the non-zero elements of the input and a small random subset of the zero elements, and to use importance sampling weights to exactly correct the bias thus introduced.

The learning objective is sampled in the following manner:

$$\hat{L}(\mathbf{x},\mathbf{z}) = \sum_k^d \frac{\hat{\mathbf{p}}_k}{\mathbf{q}_k} H(\mathbf{x}_k, \mathbf{z}_k)$$

where $\hat{\mathbf{p}} \in \{0,1\}^{d_x}$ with $\hat{\mathbf{p}} \sim P(\hat{\mathbf{p}}|\mathbf{x})$. The sampling pattern $\hat{\mathbf{p}}$ is resampled for each presentation of the input and it controls which input unit will participate in the training cost for this presentation. The bias introduced by sampling can be corrected by setting the reweighting term $1/\mathbf{q}$ such that $\mathbf{q}_k = E[\hat{\mathbf{p}}_k|k,\mathbf{x},\tilde{\mathbf{x}}]$.

The optimal sampling probabilities $P(\hat{\mathbf{p}}|\mathbf{x})$ are those that minimize the variance of the estimator $\hat{L}$. Dauphin et al. (2011) show that reconstructing all non-zeros and a small subset of zeros is a good heuristic. The intuition is that the model is more likely to be wrong on the non-zeros than the zeros. Let $\mathcal{C}(\mathbf{x},\tilde{\mathbf{x}}) = \{k : \mathbf{x}_k = 1 \text{ or } \tilde{\mathbf{x}}_k = 1\}$. Then bit k is reconstructed with probability

$$P(\hat{\mathbf{p}}_k = 1|\mathbf{x}_k) = \begin{cases} 1 & \text{if } k \in \mathcal{C}(\mathbf{x},\tilde{\mathbf{x}}) \\ |\mathcal{C}(\mathbf{x},\tilde{\mathbf{x}})|/d_x & \textit{otherwise} \end{cases} \tag{1}$$

Dauphin et al. (2011) show that the computational speed-up is on the order of ${}^{d_{SMP}}/_{d_x}$ where d_{SMP} is the average number of units that are reconstructed and d_x is the input dimension. Furthermore, reconstruction sampling yields models that converge as fast as the non-sampled networks in terms of gradient steps (but where each step is much faster).

2.3. Postprocessing

The competition servers use a Hebbian classifier. Specifically, the discriminant function applied to a test set matrix Z (one row per example) after training the representation on a training set matrix X (one row per example) is given by

$$f(Z) = ZX^T y$$

where $y_i = 1/n_p$ if training example i is positive, or $-1/n_n$ if training example i is negative, where n_p and n_n are the number of positive and negative training examples, respectively. One classifier per class (one against all) is trained.

This classifier does not have any regularization hyperparameters. We were interested in discovering whether some postprocessing of our features could result in Hebbian learning behaving as if it was regularized. It turns out that in a sense, Hebbian learning is already maximally regularized. Fisher discriminant analysis can be solved as a linear regression problem (Bishop, 2006), and the L2 regularized version of this problem yields this discriminant function:

$$g_\lambda(Z) = Z(X^T X + \lambda I)X^T y$$

where λ is the regularization coefficient. Note that

$$\lim_{\lambda \to \infty} \frac{g_\lambda(Z)}{||g_\lambda(Z)||} = \frac{f(Z)}{||f(Z)||}.$$

Since scaling does not affect the final classification decision, Hebbian learning may be seen as maximally regularized Fisher discriminant analysis. It is possible to reduce Hebbian learning's implicit L2 regularization coefficient to some smaller λ by multiplying Z by $(X^T X + \lambda I)^{-1/2}$), but it is not possible to increase it.

Despite this implicit regularization, overfitting is still an important obstacle to good performance in this competition due to the small number of training examples used. We therefore explored other means of avoiding overfitting, such as reducing the number of features and exploring sparse codes that would result in most of the features appearing in the training set being 0. However, the best results and regularization where obtained by a transductive PCA.

2.3.1. Transductive PCA

A Transductive PCA is a PCA transform trained not on the training set but on the test (or validation) set. After training the first k layers of the pipeline on the training set, we trained a PCA on top of layer k, either on the validation set or on the test set (depending on whether we were submitting to the validation set or the test set). Regarding the notation used in 2.1, we apply the same transformation with X replaced by the representation on top of layer k of the validation set or the test set i.e $h(X_{valid})$.

This transductive PCA thus only retains variations that are the dominant ones in the test or validation set. It makes sure that the final classifier will ignore the variations present in the training set but irrelevant for the test (or validation) set. In a sense, this is a generalization of the strategy introduced in 2.1 of removing features that were not present in the both training and test / validation sets. The lower layers only keep the directions of variation that are dominant in the training set, while the top transductive PCA only keeps those that are significantly present in the validation (or test) set.

We assumed that the validation and test sets contained the same number of classes to validate the number of components on the validation set performance. In general, one needs at least $k-1$ components in order to separate k classes by a set of one-against-all classifiers. Transductive PCA has been decisive for winning the competition as it improved considerably the performance on all the datasets. In some cases, we also used a mixed strategy for the intermediate layers, mixing examples from all three sets.

2.3.2. Other methods

After the feature extraction process, we were able to visualize the data as a three-dimensional scatter plot of the representation learnt. On some datasets, a very clear clustering pattern became visually apparent, though it appeared that several clouds came together in an ambiguous region of the latent space discovered.

In order to attempt to disambiguate this ambiguous region without making hard-threshold decisions, we fit a Gaussian mixture model with the EM algorithm and a small number of Gaussian components chosen by visual inspection of these clouds. We then used the posterior probabilities of the cluster assignments as an alternate encoding.

K-means, by contrast with Gaussian mixture models, makes a hard decision as to cluster assignments. Many researchers were recently impressed when they found out that a certain kind of feature representation (the "triangle code") based on K-means, combined with specialized pre-processing, yielded state of the art performance on the CIFAR-10 image classification benchmark (Coates et al., 2011). Therefore, we tried K-means with a large number of means and the triangle code as a post-processing step.

In the end, though, none of our selected final entries included a Gaussian mixture model or K-means, as the transductive PCA always worked better as a post-processing layer.

3. Criterion

The usual kind of overfitting is due to specializing to particular labeled examples. In this transfer learning context, another kind of overfitting arose: overfitting a representation to particular *classes*. Since the validation set and test set have non-intersecting sets of classes, finding representations that work well on the validation set was not a guarantee for good behavior on the test set, as we learned from our experience with the competition first phase. Note also that the competition was focused on a particular criterion, the Area under the Learning Curve (ALC)[3] which gives much weight to the cases with very few labeled examples (1, 2, or 4, per class, in particular, get almost half of the weight). So the question we investigated in the second and final phase (where some training set labels were revealed) was the following: does the ALC of a representation computed on a particular subset of classes correlate with the ALC of the same representation computed on a different set of classes?

Overfitting on a specific subset of classes can be observed by training a PCA separately on the training, validation and test sets on **ULE** (this data set corresponds to MNIST digits). The number of components maximizing the ALC will be different, depending on the choice of the subset of classes. Figure 1(a) illustrates the effect of the number of components retained on the training, validation and test ALCs. While the best number of components on the validation set would be 2, choosing this number of components for the test set significantly degrades the test ALC.

During the first phase, we noticed the absence of correlation between the validation ALC and test ALC computed on the **ULE** dataset. During the second phase, we tried to reproduce the competition setting using the labels available for transfer with the hope of finding a criteria that would guarantee generalization. The ALC was computed on every subset of at least two classes found in the transfer labels and metrics were derived. Those metrics are illustrated in Figure 1(b). We observed that the standard deviation seems to be inversely proportional to the generalization accuracy, therefore substracting it from the mean ALC ensures that the choice of hyper-parameters is done in a range where the training,

3. http://www.causality.inf.ethz.ch/ul_data/DatasetsUTLChallenge.pdf

validation and test ALCs are correlated. In the case of a PCA, optimizing the $\mu - \sigma$ criteria correctly returns the best number of PCA components, ten, where the training, validation and test ALCs are all correlated.

It appears that this criterion is a simple way to use the small amount of labels given to the competitors for the phase 2. However, this criterion has not been heavily tested during the competition since we always selected our best models with respect to the validation ALC returned by the competition servers. From the phase 1 to the phase 2, we only explored the space of the hyperparameters of our models using a finer grid.

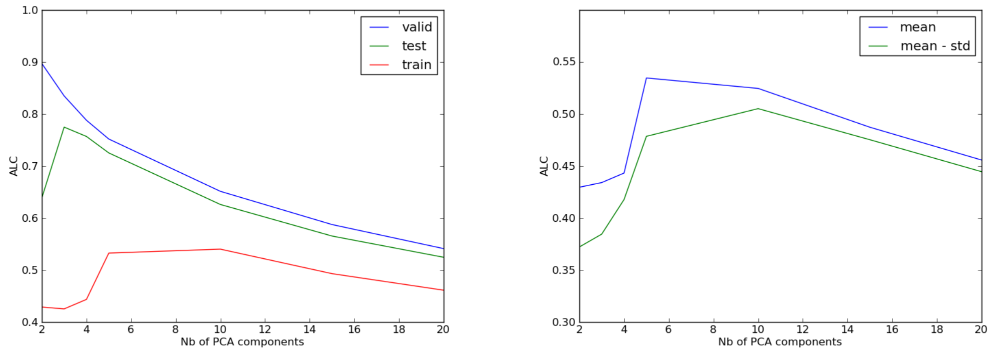

(a) ALC on the three sets

(b) Criterion

Figure 1: **ULE Dataset** Left: ALC on training, validation and test sets of PCA representations, with respect to the number of principal components retained. Right: Comparison between training, validation and test ALC and the criterion computed from the ALC, obtained on every subset of at least 2 classes present in the transfer labels for different numbers of components of a PCA.

4. Results

For each of the five datasets, **AVICENNA**, **HARRY**, **TERRY**, **SYLVESTER** and **RITA**, the strategy retained for the final winning submission on the phase 2 is precisely described. Training such a deep stack of layers from preprocessing to postprocessing takes at most 12 hours for each dataset once you have found the good hyperparameters. All our models are implemented in Theano (Bergstra et al., 2010), a Python library that allows transparent use of GPUs. During the competition, we used a cluster of GPUs, Nvidia GeForce GTX 580.

4.1. AVICENNA

Nature of the data It corresponds to arabic manuscripts and consists of 150,205 training samples of dimension 120.

Best Architecture For preprocessing, we fitted a whitened-PCA on the raw data and kept the first 75 components in order to eliminate the noise from the input distribution.

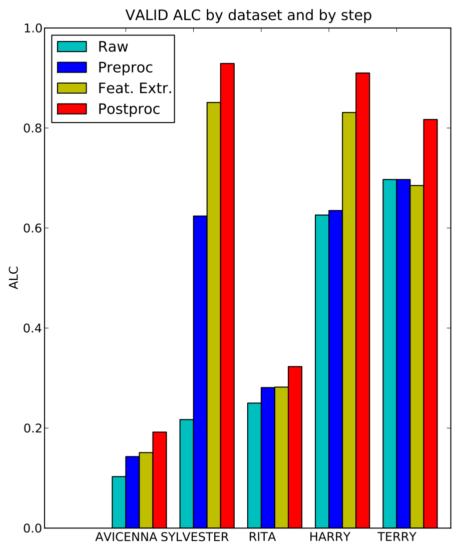

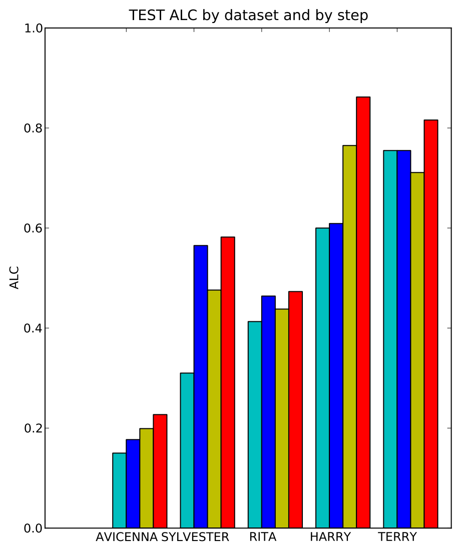

Figure 2: For each data set, we report the Validation and Test ALC after each layer (from raw data to postprocessing). It allows us to see where overfitting arose (**SYLVESTER**) and which of the layers resulted the more important to improve the overall performance.

Then, the second layer consisted in a Denoising Autoencoder of 600 hidden units trained with a binomial noise, i.e, each component of the input had a probability $p = 0.3$ of being masked (set to 0). The top layer was a transductive PCA with only the 7 principal components.

Results This strategy ranked first with a validation and final ALC score of 0.1932 and 0.2273 respectively. Training a contractive auto-encoder gives similar results on the validation set i.e a validation and final ALC score of 0.1930 and 0.1973 respectively.

4.2. HARRY

Nature of the data It corresponds to human actions and consists of $69,652$ training samples of dimension $5,000$, which are sparse: only 2% of the components are typically non-zero.

Best Architecture For the first layer, we uniformized the non-zero feature values (aggregating all features) across the concatenation of the training, validation and test sets. For the second layer, we trained on the union of the 3 sets a Denoising Auto-Encoder with rectifier units and reconstruction sampling. We used the binomial masking noise ($p = 0.5$) as corruption process, the logistic sigmoid as reconstruction activation function and the cross entropy as reconstruction error criterion. The size of the hidden layer was 5000 and

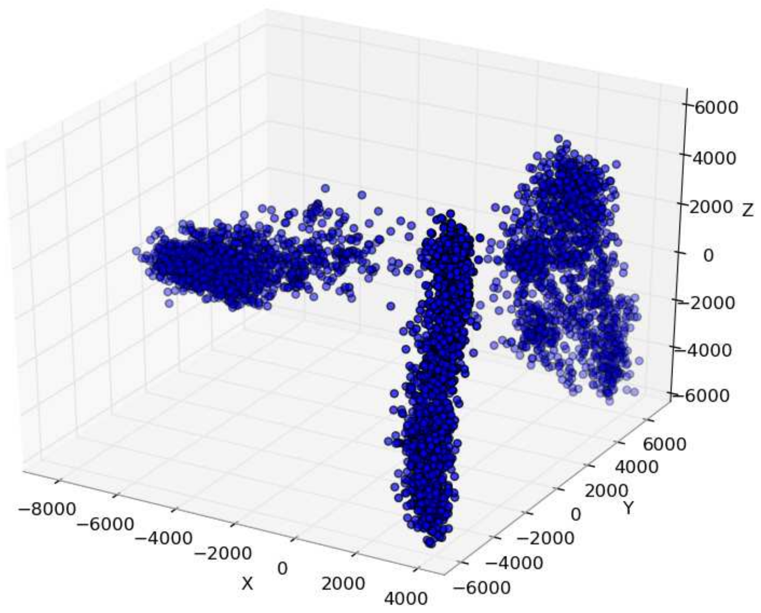

Figure 3: **HARRY** evaluation set after the transductive PCA, the data is nicely clustered, suggesting that the learned preprocessing has discovered the underlying class structure.

we added an L_1 penalty on the activation values to encourage sparsity of the representation. For the third layer, we applied a transductive PCA and kept 3 components.

Results We obtained the best validation ALC score of the competition. This was also the case for the final evaluation score with an ALC score of 0.861933, whereas the second best obtained 0.754497. Figure 3 shows the final data representation we obtained for the test (evaluation) set.

4.3. TERRY

Nature of the data This is a natural language processing (NLP) task, with 217, 034 training samples of dimension 41, 236, and a high level of sparsity: only 1% of the components are non-zero in average.

Best Architecture A setup similar to **HARRY** has been used for **TERRY**. For the first layer, we kept only the features that were active on both training and validation sets (and similarly with the test set, for preparing the test set representations). Then, we divided the non-zero feature values by their standard deviation across the concatenation of the training, validation and test set. For the second layer, we trained on the three sets a Denoising Auto-Encoder with rectifier units and reconstruction sampling. We used binomial masking noise ($p = 0.5$) as corruption process, the logistic sigmoid as reconstruction activation function and the squared error as reconstruction error criterion. The size of the hidden layer was 5000 and we added an L_1 penalty on the activation values to encourage sparsity of the representation. For the third layer, we applied a transductive PCA and kept the leading 4 components.

Results We ranked second on this dataset with a validation and final score of 0.816752 and 0.816009.

4.4. SYLVESTER

Nature of the data It corresponds to ecology data and consists of $572,820$ training samples of dimension 100.

Best Architecture For the first layer, we extracted the meaningful features and discarded the apparent noise dimensions using PCA. We used the first 8 principal dimensions as the feature representation produced by the layer because it gave the best performance on the validation set. We also whitened this new feature representation by dividing each dimension by its corresponding singular value (square root of the eigenvalue of the covariance matrix, or corresponding standard deviation of the component). Whitening gives each dimension equal importance both for the classifier and subsequent feature extractors. For the second and third layers, we used a Contractive Auto-Encoder (CAE). We have selected a layer size of 6 based on validation ALC. For the fourth layer, we again apply a transductive PCA.

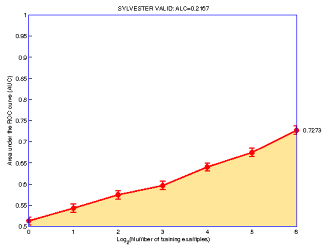

(a) Raw Data

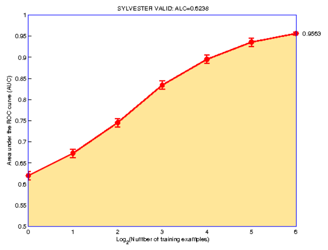

(b) 1st Layer

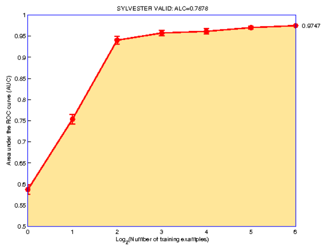

(c) 2nd Layer

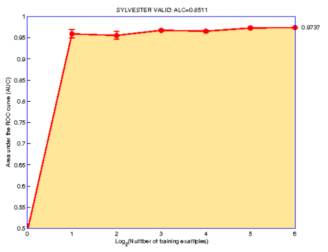

(d) 3rd Layer

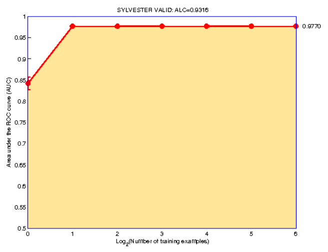

(e) t-PCA

Figure 4: Validation performance increases with the depth of our feature hierarchy for the **SYLVESTER** dataset. ALC: Raw Data (0.2167), 1st Layer (0.6238), 2nd Layer (0.7878), 3rd Layer (0.8511), t-PCA(0.9316)

Figure 4 shows the evolution of the ALC curve for each layer of the hierarchy. Note that at each layer, we only use the top-level features as the representation.

Results This yielded an ALC of 0.85109 for the validation set and 0.476341 for the test set. The difference in ALC may be explained by the fact that Sylvester is the only dataset where the test set contains more classes than the validation set and, and thus our assumpptions of equal number of classes might have hurt test performance here.

4.5. RITA

Nature of the data It corresponds to the CIFAR RGB image dataset and consists of $111,808$ training samples of dimension $7,200$.

Best Architecture The μ-ssRBM was initially developed as a model for natural images. As such, it was a natural fit for the **RITA** dataset. Their ability to learn the pooling structure was also a clear advantage, since the max-pooling strategy typically used in vision tasks with convolutional networks LeCun et al. (1998) could no longer be employed due to the obfuscated nature of the dataset.

For pre-processing, each image has been contrast-normalized. Then, we reduced the dimensionality of the training dataset by learning on the first $1,000$ principal components. For feature extraction, we chose the number of hidden units to be large enough (1000) while still being computationally efficient on GPUs. The learning rate of 10^{-3} and number of training updates ($110,000$ updates with minibatches of size 16) are chosen such that hidden units have sparse activations through pools of size 9, hovering around 10-25%. The post-processing was consistent with the other datasets: we used the transductive PCA method using only the first 4 principal components.

Results This yielded an ALC score of 0.286 and 0.437 for the validation and final test sets respectively. We also tried to stack 3 layers of contractive auto-encoders directly on the raw data and it achieved a valid ALC of 0.3268. As it appeared actually transductive, we prefered to keep the μ-ssRBM in our competition entries because it was trained on the whole training set.

5. Conclusion

The competition setting with different class labels in the validation and the test sets was quite unusual. The similarity between two classes must be sufficient for transfer learning to be possible. More formal assessments of class similarity might be useful in such settings. It is not obvious that the similarity between the subsets of classes chosen for the different datasets in the context of the competition is sufficient for an effective generalization, neither that the similarity between the subsets of classes found in the transfer labels is representative of the similarity between the classes found in the training, validation and test datasets. Finally, for assessing transfer across classes properly would require a larger number of classes. In a future competition, we suggest that both similarity and representativeness (including number of classes) should be ensured in a more formal or empirical way.

On all five tasks, we have found the idea of stacking different layer-wise representation-learning algorithms to work very well. One surprise was the effectiveness of PCA both as a first layer and a last layer, in a transductive setting. As core feature-learning blocks, the contractive auto-encoder, the denoising auto-encoder and spike-and-slab RBM worked best for us on the dense datasets, while the sparse rectifier denoising auto-encoder worked best on the sparse datasets.

Acknowledgements

The authors acknowledge the support of the following agencies for research funding and computing support: NSERC, RQCHP, CIFAR. This is also funded in part by the French ANR Project ASAP ANR-09-EMER-001.

References

Yoshua Bengio. Learning deep architectures for AI. *Foundations and Trends in Machine Learning*, 2(1):1–127, 2009. Also published as a book. Now Publishers, 2009.

Yoshua Bengio. Deep learning of representations for unsupervised and transfer learning. In *Workshop on Unsupervised and Transfer Learning (ICML'11)*, June 2011.

Yoshua Bengio, Pascal Lamblin, Dan Popovici, and Hugo Larochelle. Greedy layer-wise training of deep networks. In Bernhard Schölkopf, John Platt, and Thomas Hoffman, editors, *Advances in Neural Information Processing Systems 19 (NIPS'06)*, pages 153–160. MIT Press, 2007.

James Bergstra, Olivier Breuleux, Frédéric Bastien, Pascal Lamblin, Razvan Pascanu, Guillaume Desjardins, Joseph Turian, David Warde-Farley, and Yoshua Bengio. Theano: a CPU and GPU math expression compiler. In *Proceedings of the Python for Scientific Computing Conference (SciPy)*, June 2010. URL http://www.iro.umontreal.ca/~lisa/pointeurs/theano_scipy2010.pdf. Oral.

Christopher M. Bishop. *Pattern Recognition and Machine Learning.* Springer, 2006.

A. Coates, H. Lee, and A. Ng. An analysis of single-layer networks in unsupervised feature learning. In *Proceedings of the Thirteenth International Conference on Artificial Intelligence and Statistics (AISTATS 2011)*, 2011.

Aaron Courville, James Bergstra, and Yoshua Bengio. Unsupervised models of images by spike-and-slab RBMs. In *Proceedings of the Twenty-eight International Conference on Machine Learning (ICML'11)*, June 2011.

Yann Dauphin, Xavier Glorot, and Yoshua Bengio. Sampled reconstruction for large-scale learning of embeddings. In *Proceedings of the Twenty-eight International Conference on Machine Learning (ICML'11)*, June 2011.

Xavier Glorot, Antoire Bordes, and Yoshua Bengio. Deep sparse rectifier neural networks. In *JMLR W&CP: Proceedings of the Fourteenth International Conference on Artificial Intelligence and Statistics (AISTATS 2011)*, April 2011.

Y. LeCun, L. Bottou, Y. Bengio, and P. Haffner. Gradient based learning applied to document recognition. *IEEE*, 86(11):2278–2324, November 1998.

V. Nair and G. E Hinton. Rectified linear units improve restricted Boltzmann machines. In *Proc. 27th International Conference on Machine Learning*, 2010.

M. Ranzato and G. H. Hinton. Modeling pixel means and covariances using factorized third-order Boltzmann machines. In *Proceedings of the Computer Vision and Pattern Recognition Conference (CVPR'10)*, pages 2551–2558. IEEE Press, 2010.

Salah Rifai, Pascal Vincent, Xavier Muller, Xavier Glorot, and Yoshua Bengio. Contractive auto-encoders: Explicit invariance during feature extraction. In *Proceedings of the Twenty-eight International Conference on Machine Learning (ICML'11)*, June 2011.

Tijmen Tieleman. Training restricted Boltzmann machines using approximations to the likelihood gradient. In William W. Cohen, Andrew McCallum, and Sam T. Roweis, editors, *Proceedings of the Twenty-fifth International Conference on Machine Learning (ICML'08)*, pages 1064–1071. ACM, 2008.

Pascal Vincent, Hugo Larochelle, Yoshua Bengio, and Pierre-Antoine Manzagol. Extracting and composing robust features with denoising autoencoders. In William W. Cohen, Andrew McCallum, and Sam T. Roweis, editors, *Proceedings of the Twenty-fifth International Conference on Machine Learning (ICML'08)*, pages 1096–1103. ACM, 2008.

Pascal Vincent, Hugo Larochelle, Isabelle Lajoie, Yoshua Bengio, and Pierre-Antoine Manzagol. Stacked denoising autoencoders: Learning useful representations in a deep network with a local denoising criterion. *Journal of Machine Learning Research*, 11(3371–3408), December 2010.